Molecular Crystals and Liquid Crystals
Publication details, including instructions for authors and subscription information:
http://www.tandfonline.com/loi/gmcl20

Thermotropic Mesomorphic and Odd-Even Melting Behavior of a Homologous Series of Zinc(II) n-Alkanoates

Richard A. Taylor [a] & Henry A. Ellis [a]

[a] Department of Chemistry, Faculty of Pure and Applied Sciences, The University of the West Indies, Jamaica, West Indies

Version of record first published: 07 Oct 2011

To cite this article: Richard A. Taylor & Henry A. Ellis (2011): Thermotropic Mesomorphic and Odd-Even Melting Behavior of a Homologous Series of Zinc(II) n-Alkanoates, Molecular Crystals and Liquid Crystals, 548:1, 37-54

To link to this article: http://dx.doi.org/10.1080/15421406.2011.590351

Mol. Cryst. Liq. Cryst., Vol. 548: pp. 37–54, 2011

ISSN: 1542-1406 print/1563-5287 online
DOI: 10.1080/15421406.2011.590351

Taylor & Francis
Taylor & Francis Group

Thermotropic Mesomorphic and Odd–Even Melting Behavior of a Homologous Series of Zinc(II) *n*-Alkanoates

RICHARD A. TAYLOR* AND HENRY A. ELLIS

Department of Chemistry, Faculty of Pure and Applied Sciences, The University of the West Indies, Jamaica, West Indies

The thermotropic phase behavior of a series of odd-chain polymeric zinc(II) n-*alkanoates, $Zn(C_nH_{2n-1}O_2)_2$ [$ZnC_{5–19}$], is studied by differential scanning calorimetry (DSC) and temperature variation polarizing light microscopy and compared with data of even-chain homologues. The compounds exhibit both enantiotropic and monotropic phase behavior on heating to the isotropic liquid and on cooling back to the room-temperature solid:*

$ZnC_{5–11}$; Lamellar crystal ↔ Crystal I ↔ Crystal II ↔ Isotropic melt;
$ZnC_{13–15}$; Lamellar crystal ↔ Crystal I ↔ Isotropic liquid;
$ZnC_{17–19}$; Lamellar crystal → Isotropic liquid (heating)

"Smectic C-like" Lamellar crystal ← Smectic C ← Isotropic liquid (cooling)
Odd–even behavior is observed in the thermodynamic data and is attributed to the difference in the packing efficiency of odd- and even-numbered hydrocarbon chains within the lattice. The thermodynamic data along with solid-state infrared (IR) and X-ray diffraction data suggest that electrostatic interactions play a prominent role in the melting process in addition to fusion of the alkyl chains. An equilibrium model is proposed as the structure for the isotropic melt.

Keywords: Odd–even behavior; thermotropic phase behavior; zinc(II) *n*-alkanoates

1. Introduction

Mesogenic behavior of metal carboxylates has been an important area of study for many decades, particularly since many of them exhibit the smectic C (Sm C) mesophase, in which the molecules form a layered structure with the molecular long axes being tilted with respect to the layer normal [1], and as such, have potential use in ferroelectric liquid crystal displays (LCDs). As a result, the study of the thermotropic phase transition behavior of various monovalent and divalent metal carboxylates has been a focus of this field of research [2–13]. Of keen interest is the homologous series of zinc(II) *n*-alkanoates, and related studies involved a comprehensive proposal of their room-temperature molecular and lattice structures [14,15], and most recently, a report of conclusive data on the phase behavior of the even-chain homologues [16]. As with materials in the solid state, there is a clear correlation between structural features and their properties, and for compounds that

*Address correspondence to Department of Chemistry, Faculty of Science and Agriculture, The University of the West Indies, St. Augustine, Trinidad and Tobago, West Indies. E-mail: richard.taylor@sta.uwi.edu

display thermotropic mesomorphism, there must be a firm understanding of the relationship between structure, intermolecular interactions, and thermophysical properties and the phase behavior.

As reported previously [16], a combination of differential scanning calorimetry (DSC) data and microscopic phase textures indicated that a homologous series of even-chain Zn(II) *n*-alkanoates, from the butanoate to eicosanoate (ZnC_4–ZnC_{20}) inclusive, displayed both enantiotropic and monotropic phase behavior, in which there was some relationship between the number of phases observed and the chain length, which was ascribed to the possible difference in lattice structures of the starting solid material. For example, on heating the short- and medium-chain compounds, only solid-to-solid transitions occurred, but interestingly, on cooling from the isotropic melt, a kinetically controlled Sm C mesophase appeared for the long-chain ZnC_{18} and ZnC_{20}. Data of enthalpy change (ΔH_{fusion}) and entropy change (ΔS_{fusion}) for fusion suggested that electrostatic interactions in the polar region played an important role in the melting process, in addition to fusion of the hydrocarbon chains being the major part, leading to an isotropic melt with very few or no micellar aggregates.

In the study [14,15] of the room-temperature molecular and lattice structures, it was clearly shown that there was an odd–even behavior in the packing of the hydrocarbon chains. In order to understand what was the basis of this odd–even behavior, spectroscopic data of the infrared (IR) anti-symmetric stretch of the methyl group, $\nu_a(CH_3)$, and the solid-state ^{13}C NMR (nuclear magnetic resonance) chemical shift, δ, values for the methyl carbon were presented, which also displayed the odd–even variation. These data also complimented the odd–even variation in the density and melting point data, which clearly pointed to a difference in the hydrocarbon chain packing in the lattice [14,15]. The data strongly suggested that CH_3 groups of the even-chain homologues were in close proximity to the Zn^{2+} ion, pointing into the basal plane of the Zn^{2+} ion lattice, as opposed to the odd-chain homologues, which pointed along the basal plane, resulting in a less close approach to the Zn^{2+} ion. Proposed molecular models showed that the even-chain homologues had a higher packing efficiency, accounting for the higher density and melting point than the odd-chain homologues. It is clear then that since electrostatic interactions played an important role in the melting behavior of the even-chain homologues, it would be important to show whether or not these interactions are different in the odd- and even-chain homologues, thereby showing an odd–even variation in the phase transition or melting process for the entire homologous series.

Based on these previous studies, this paper seeks to present additional data from DSC for the thermotropic phase transition behavior of odd-chain Zn(II) *n*-alkanoates. The DSC thermodynamic data are compared with previously presented DSC data for the even-chain homologues to determine whether there is any odd–even behavior. This will allow for a thorough structural and thermophysical interpretation of the basis for the odd–even behavior of these compounds, which may also be useful for other metal carboxylates that exhibit this behavior. IR and X-ray data of compounds that are heated to the isotropic liquid and cooled back to room temperature are compared with data from unheated compounds to provide evidence for the role of electrostatic interactions during the melting process. Finally, a complete picture of the melting process is presented with thermodynamic analysis of the nature of the isotropic liquid.

2. Experimental

The preparation, purification, and confirmation of the purity of the odd-chain Zn(II) *n*-alkanoates have been previously described [14,17]. Measurement of DSC phase profiles

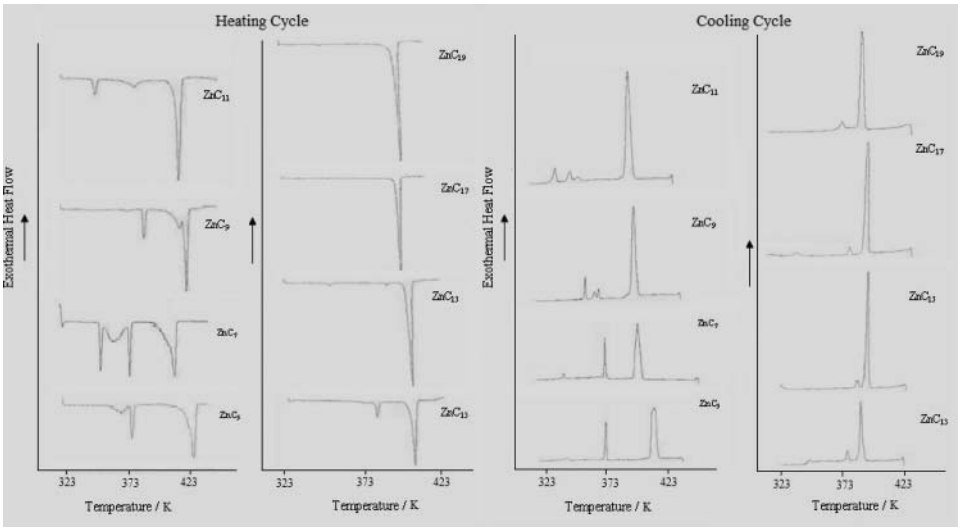

Figure 1. DSC thermograms for the first heating and cooling cycles of odd-chain zinc(II) *n*-alkanoates.

along with thermodynamic data and microscopic phase textures of freshly prepared compounds have been previously described [16].

Additionally, IR spectroscopic and X-ray diffraction analyses (previously described [14,17]) were carried out on selected compounds, which were placed in ceramic crucibles and heated in air at 2.0 K min^{-1} from room temperature to approximately 5 K above their melting point in an oven, followed by immediate cooling back to room temperature.

3. Results and Discussion

3.1 Phase Transitions

DSC phase transition scans for the odd-chain Zn(II) *n*-alkanoates over a temperature range of 323.0 K–443.0 K at a scan rate of 2.0 K min^{-1} are shown in Fig. 1. As with the even-chain homologues [16], one or more endothermic phase transitions occur between the solid and the isotropic liquid on first heating, and there appears to be some relationship between the number of phases observed and the chain length. The compounds were immediately cooled at a scan rate of 2.0 K min^{-1} from the isotropic liquid to 323.0 K. Similar to the even-chain homologues [16], one or more exothermic transitions are observed, as shown in Fig. 1. As in the heating scan, there are distinct differences observed for short- and long-chain homologues.

Polarized light microscopy was used to identify and confirm the various phases for odd-chain $ZnC_{5–19}$. For example, $ZnC_{5–15}$ phase textures, shown in Figs. 2(a) and (b), obtained on cooling into the phases, are highly viscous, birefringent, and resistant to a sheer stress applied to the microscope slide, similar to phase textures for the even-chain homologues [16]. This is clearly an indication of crystal-to-crystal phase transitions only, between the room-temperature solid and isotropic liquid. Moreover, the brightly colored radiating textures are typical for crystalline structures and appear similar to each other, suggesting no significant change in structure between phases, and are similar to those obtained for the

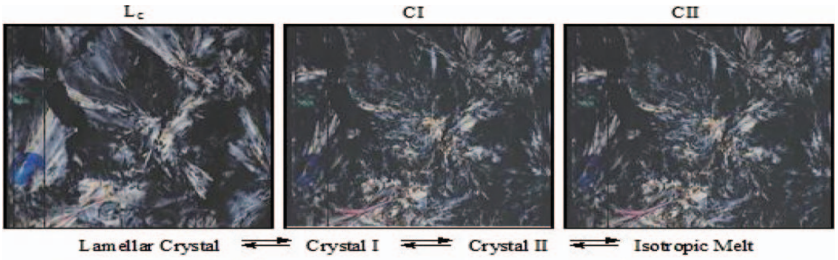

(a) Phase sequence for ZnC_{5-11} for first heating – cooling cycle; ZnC_5 shown as an example.

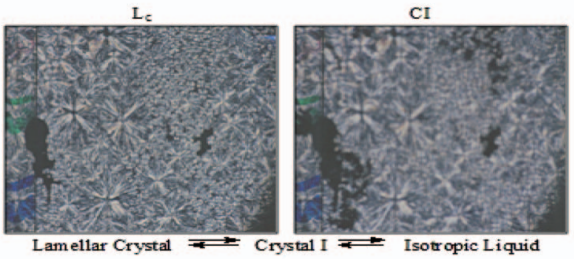

(b) Phase sequence for ZnC_{13-15} for first heating – cooling cycle; ZnC_{15} shown as an example.

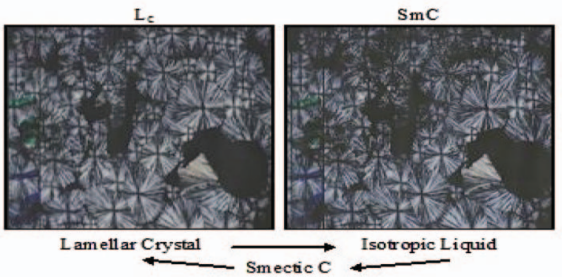

(c) Phase sequence for ZnC_{17-19} for first heating – cooling cycle; ZnC_{19} shown as an example.

Figure 2. Representative microscopic phase textures along with phase sequences for zinc(II) *n*-alkanoates.

even-chain homologues [16]. In addition, they appear similar to the exotherms in the DSC scans. Additionally, the transitions are reversible, i.e., they exhibit enantiotropic phase behavior. However, the long-chain homologues, ZnC_{17} and ZnC_{19}, exhibit monotropic phase behavior similar to ZnC_{18} and ZnC_{20} [16], as shown in Fig. 2(c). This involves direct transition from the lamellar crystal (L_C) to the melt on heating, but on cooling from the melt, a very fast, almost imperceptible transition to an Sm C phase is observed, as demonstrated by the broken fan textures which appeared on forming the phases. The change back to the lamellar crystal at room temperature is very gradual and probably kinetically controlled, since the room-temperature texture retains many of the characteristics of the preceding Sm C texture. This is not unusual and has been reported for other compounds [18]. Since the phase did not return to the normal lamellar crystal, this phase at room temperature is described as a "smectic C-like" crystal.

The "heated and then cooled" compounds are immediately reheated at 2.0 K min^{-1} in order to check for reproducibility in DSC transition peaks. They are generally similar to

those initially obtained on first heating. On cooling a second time, one or more exotherms are observed for the series and are fairly similar to those in the first cooling scan. The similarity in the phase profiles in the first and second cycles suggests that there may be no significant changes in the molecular structure after heating and cooling these compounds and that the heating–cooling cycle is fairly reversible. Overall, the phase profiles are similar to those of the even-chain homologues [16].

3.2 Odd–Even Melting Behavior

It has been established that for metal carboxylates, the molar enthalpy change associated with the fusion process can be decomposed based on energy contributions as follows [16, 19, 20]:

$$\Delta_{\text{fusion}}H = \Delta U_{\text{conf}} + \Delta U_{\text{vdW}} + \Delta U_{\text{o}} + \text{p}\Delta V, \tag{1}$$

where ΔU_{conf} and ΔU_{vdW} are energy changes associated with intramolecular conformational disorder (i.e., introduction of gauche conformations in the chains during melting) and intermolecular van der Waals interactions, respectively. ΔU_{o} incorporates energy changes associated with electrostatic interactions, and $\text{p}\Delta V$, the energy associated with changes in the molar volume, is small compared with the others and can be neglected.

The DSC thermodynamic data for transition temperatures, T_{trans}, molar enthalpy of transition, ΔH_{trans}, total molar enthalpy change, ΔH_{total}, molar entropy of transition, ΔS_{trans}, and total molar entropy change, ΔS_{total} are given in Tables 1 and 2 for the first and second heating scans for the odd-chain compounds, respectively, in addition to the previously reported data for even-chain compounds [16], to show any odd–even trends. Plots of ΔH_{fusion} and $\Delta \text{S}_{\text{fusion}}$ against chain length, n_{c} in Fig. 3 for the first and second heating scans show strong linear correlations for both odd- and even-chain homologues. Values of the slopes and intercepts obtained from the good linear correlations (fitted to Equation (2)) are summarized in Table 3.

$$\Delta H_{\text{fusion}}[\text{Zn}(\text{O}_2\text{C})(\text{CH}_2)_n(\text{CH}_3)] = n\Delta H_{\text{fusion}}(\text{CH}_2) + \Delta H_{\text{fusion}}[\text{CH}_3^- + (\text{CO}_2)\text{Zn}]. \tag{2}$$

The slopes of the lines indicate the contribution from a single CH_2 group to the interchain interactions, while the intercepts represent the enthalpies of rearrangement of the bonds between the Zn^{2+} ion and the carboxylate (COO^-) groups as well as the interactions between the polar (Zn–OOC) and the terminal CH_3 groups in the molecular and lattice structures. For each heating scan, slopes for the odd- and even-chain homologues for ΔH_{fusion} plots given in Table 3 are fairly similar and suggest that the contribution of the CH_2 groups to the enthalpy of melting of the chains is fairly similar. Accordingly, the linear increase in the overall enthalpy of fusion with chain length and the fairly large slope values, which are almost twice as large the value 7.60 kJ mol^{-1} per CH_2 obtained for complete fusion of the alkanoic acids in their fully crystalline dimeric state [21], are associated with both the decrease in the van der Waals interactions between the hydrocarbon chains and the introduction of some degree of conformational disorder where the orientation of the CH_2 groups of the hydrocarbon chains has changed from all-*trans* to a high degree of gauche conformation during melting. Since the chains are fully fused, it suggests that the melt has little or no structural order, with few or no micellar aggregates, as proposed for the even-chain homologues [16] and other metal carboxylates [20, 22, 23].

Table 1. DSC thermodynamic data from the first heating scan for zinc(II) *n*-alkanoates

	Lamellar crystal, L_C–Phase I			Phase I–Phase II			L_C/Phases I/II–Isotropic liquid			Total		
Compound	T (±1.3 K)	ΔH_{trans} (±0.09 kJ mol^{-1})	ΔS_{trans} (±0.25 J K^{-1} mol^{-1})	T (±1.4 K)	ΔH_{trans} (±0.16 kJ mol^{-1})	ΔS_{trans} (±0.41 J K^{-1} mol^{-1})	T (±1.5 K)	ΔH_{trans} (±1.40 kJ mol^{-1})	ΔS_{trans} (±3.43 J K^{-1} mol^{-1})	ΔH_{total} (±1.51 kJ mol^{-1})	ΔS_{total} (±5.14 J K^{-1} mol^{-1})	Reference
ZnC_4	364.2	4.24	11.46	377.8	10.10	26.72	428.6	40.96	95.57	55.30	133.76	[5]
ZnC_5	369.2	*	*	377.7	17.41	46.10	425.4	40.73	95.76	58.14	141.86	This work
ZnC_6	356.1	13.69	38.44	379.2	9.81	25.87	419.2	48.83	116.48	72.33	180.79	[5]
ZnC_7	355.1	10.49	29.53	378.1	9.72	25.71	412.1	31.75	77.07	51.96	132.31	This work
ZnC_8	373.3	2.89	1.74	395.4	21.51	54.39	412.2	76.60	185.83	103.07	241.96	[5]
ZnC_9	369.8	2.14	5.79	382.5	16.90	44.12	412.0	84.03	203.96	103.07	253.87	This work
ZnC_{10}	372.9	3.05	15.20	385.9	17.84	46.24	408.4	91.89	225.08	112.78	286.52	[5]
ZnC_{11}	347.1	10.87	31.33	374.1	11.13	29.78	405.1	92.23	227.67	114.23	288.78	This work
ZnC_{12}	376.2	3.20	8.55	–	–	–	405.9	140.68	346.63	143.88	355.18	[5]
ZnC_{13}	379.8	22.60	59.60	–	–	–	402.9	106.68	264.88	129.28	324.48	This work
ZnC_{14}	383.8	12.10	31.51	–	–	–	404.8	152.43	376.56	164.53	408.07	[5]
ZnC_{15}	389.2	6.47	16.63	–	–	–	403.2	175.82	436.12	182.29	452.75	This work
ZnC_{16}	–	–	–	–	–	–	405.7	205.07	505.47	205.07	505.47	[5]
ZnC_{17}	–	–	–	–	–	–	403.8	214.63	531.53	214.63	531.53	This work
ZnC_{18}	–	–	–	–	–	–	406.7	235.47	578.98	235.47	578.98	[5]
ZnC_{19}	–	–	–	–	–	–	403.7	218.73	541.88	218.73	541.88	This work
ZnC_{20}	–	–	–	–	–	–	406.1	232.64	572.93	232.64	572.93	[5]

*Values could not be determined because endotherm could not be separated from proceeding endotherm.

Table 2. DSC thermodynamic data from the second heating scan for zinc(II) *n*-alkanoates

	Lamellar crystal, L_C–Phase I			Phase I–Phase II			L_c/Phases I/II–Isotropic liquid			Total		
Compound	T (±0.5 K)	ΔH_{trans} (±0.19 kJ mol^{-1})	ΔS_{trans} (±0.51 J K^{-1} mol^{-1})	T (±0.5 K)	ΔH_{trans} (±0.14 kJ mol^{-1})	ΔS_{trans} (±0.37 J K^{-1} mol^{-1})	T (±1.5 K)	ΔH_{trans} (±2.32 kJ mol^{-1})	ΔS_{trans} (±5.78 J K^{-1} mol^{-1})	ΔH_{total} (±1.51 kJ mol^{-1})	ΔS_{total} (±5.14 J K^{-1} mol^{-1})	Reference
ZnC_4	356.1	2.08	5.85	377.3	9.53	25.27	429.0	45.87	106.92	57.49	138.04	[16]
ZnC_5	353.6	*	*	377.1	7.66	20.31	427.1	39.98	93.62	47.64	113.93	This work
ZnC_6	366.9	1.55	4.22	378.0	11.51	30.45	418.8	47.42	113.22	60.48	147.89	[16]
ZnC_7	353.2	7.15	20.20	377.7	9.67	25.61	414.1	47.99	115.89	64.81	161.70	This work
ZnC_8	378.5	10.03	26.49	386.4	4.80	12.43	411.3	72.65	176.66	87.48	215.58	[16]
ZnC_9	363.7	7.13	19.62	381.7	1.65	4.32	409.7	82.32	200.93	91.10	224.87	This work
ZnC_{10}	372.3	11.17	30.00	384.7	4.53	11.77	408.3	81.93	200.69	97.63	242.46	[16]
ZnC_{11}	341.8	7.17	20.98	355.4	2.31	5.50	404.5	86.73	214.43	96.21	240.91	This work
ZnC_{12}	366.7	16.70	45.56	375.0	5.21	13.88	405.2	99.49	245.56	121.40	305.00	[16]
ZnC_{13}	377.6	11.37	30.11	–	–	–	402.3	111.99	278.41	123.36	308.52	This work
ZnC_{14}	381.7	6.39	16.74	–	–	–	402.6	111.19	276.18	117.58	292.92	[16]
ZnC_{15}	386.0	14.33	37.15	–	–	–	403.5	136.96	339.43	151.29	376.58	This work
ZnC_{16}	–	–	–	–	–	–	403.3	164.72	408.48	164.72	408.48	[16]
ZnC_{17}	–	–	–	–	–	–	401.8	165.86	412.84	165.86	412.84	This work
ZnC_{18}	–	–	–	–	–	–	401.1	171.78	428.27	171.78	428.27	[16]
ZnC_{19}	–	–	–	–	–	–	400.5	137.17	342.50	137.17	342.50	This work
ZnC_{20}	–	–	–	–	–	–	403.9	205.07	507.79	205.07	507.79	[16]

*Values could not be determined because endotherm could not be separated from proceeding endotherm.

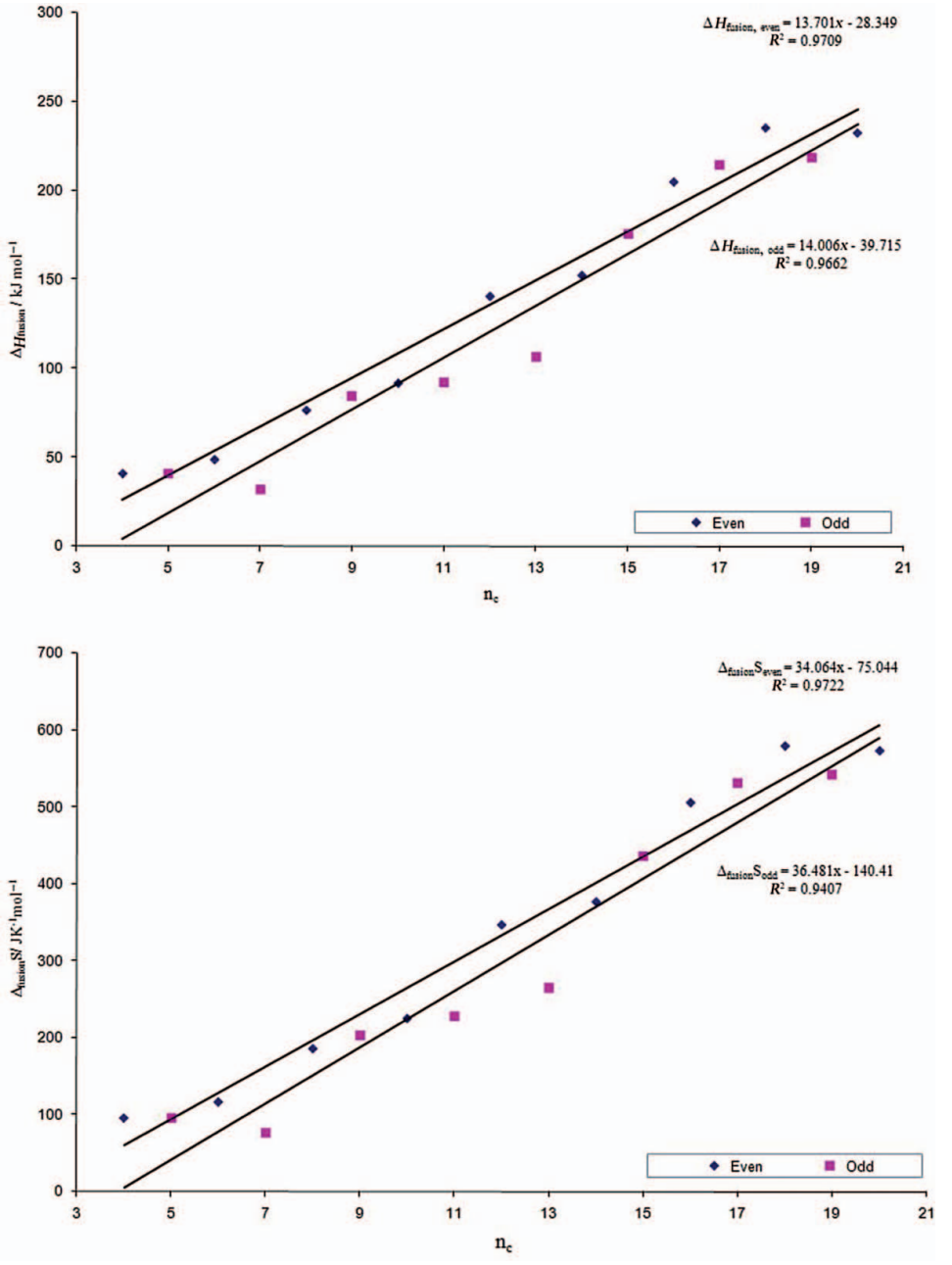

Figure 3. Plots of ΔH_{fusion} and ΔS_{fusion} versus n_c for first and second heating scans of the homologous series.

Additionally, extrapolation to zero CH_2 groups of the ΔH_{fusion} versus n_c plots gives intercepts of -39.72 and -28.35 kJ mol^{-1} for odd- and even-chain homologues, respectively, which imply a distinct odd–even effect, as seen in the difference in the plots. Since the thermophysical contribution of CH_2 groups during the melting process is not expected

Table 3. Calculated values for slope and intercept from linear plots of ΔH and ΔS versus n_c for heating scans

		Slope (kJ mol^{-1})		Intercept (J K^{-1} mol^{-1})	
Scan	Type of graph	Odd	Even	Odd	Even
1	ΔH_{fusion}	14.01	13.70	−39.72	−28.35
2	ΔH_{fusion}	10.45	10.39	−18.98	−10.95
1	ΔH_{total}	11.97	12.12	−5.49	1.77
2	ΔH_{total}	10.02	9.36	−4.29	10.8
1	ΔS_{fusion}	38.11	34.06	−105.18	−75.04
2	ΔS_{fusion}	26.47	26.2	−54.64	−34.4
1	ΔS_{total}	32.31	30.00	−54.32	2.65
2	ΔS_{total}	24.93	23.46	−10.48	23.51
Reference		This study	[5]	This study	[5]

to account for the difference in the intercept values from the plots, it would be reasonable to assume that the difference is directly related to the difference in the interplay of the electrostatic interactions arising from the difference in the packing arrangement of odd- and even-chain homologues. It has been firmly established from previously reported spectroscopic data and proposed models [14] that the odd–even effect is likely to be related to the contribution from the CH_3 groups and the extent of their interaction with the basal plane of the Zn^{2+} ion lattice, which confirms that the even-chain homologues have a higher packing efficiency, and therefore, the lattice network would be more difficult to disrupt on heating and hence would have a less negative contribution to the fusion process than the odd-chain homologues. Also, in the basal planes of the Zn^{2+} ion lattice, Zn^{2+} ions would be repulsive toward each other and the higher packing efficiency for the even-chain homologues would counter these repulsive electrostatic interactions between them to a greater degree than in the case of odd-chain homologues, as they have a lower packing efficiency.

Furthermore, the intercept values of −39.72 and −28.35 kJ mol^{-1} from the ΔH_{fusion} versus n_c plots for odd-and even-chain homologues, respectively, imply that electrostatic interactions give a fairly strong negative contribution to the fusion process, as in the case of cerium(III) alkanoates [19]. Indeed, when the compounds melt, repulsive electrostatic interactions between Zn^{2+} ions as well as possible dipole–dipole repulsions between COO^- groups are reduced, leading to a stabilization of the system. Relaxation of the lattice may be accompanied by a change at the polar head groups, i.e., there may be some fusion of the polar region, leading to a perturbation in the COO–Zn interaction. It is possible that there may also be some breaking of the COO–Zn bonds. This is in accord with the IR data provided by Mesubi [24], which indicated that there is a change in the coordination structure on heating from solid to liquid and then cooling back to solid.

In order to understand the nature of the heating–cooling process and the thermophysical factors responsible, an analysis of the thermodynamic data from the reheating and cooling scans is germane. Interestingly, the data of the melting transition obtained from the second heating scan, tabulated in Table 2, are almost similar to those from the first heating scan, though in the second scan, the values are somewhat lower. Also, linear plots of ΔH_{fusion} versus n_c result in two sets of lines with similar slope values for odd- and even-chain homologues, the data for which are tabulated in Table 3. These slope values are somewhat

lower than those for the first cycle, but still higher than the value of 7.60 kJ mol^{-1} per CH_2 for complete fusion of the dimeric alkanoic chains. The lower values in the second scan can be attributed to some modification of the hydrocarbon chains in the lattice. Clear differences are seen in the intercept values of −18.98 and −10.95 J K^{-1} mol^{-1} for ΔH_{fusion} plots and −4.22 and 10.80 J K^{-1} mol^{-1} for ΔH_{total} plots for odd- and even-chain homologues, respectively, indicating an odd–even effect. These intercept values are larger than those of the first cycle and suggest that in the melting process, electrostatic interactions between the Zn^{2+} ions and the CH_3 groups are a significant contributory factor, which are slightly lower in the structures formed after initial heating and cooling.

Similar trends are observed for the corresponding ΔS_{fusion} and ΔS_{total} versus n_c plots for the second heating scan, as for the first heating scan; the odd–even behavior is maintained, where there are two lines for the odd- and even-chain homologues, with similar slopes for the fusion process and for the total change from solid to liquid. The values are slightly smaller but approximately the same as those for the first cycle. However, for the ΔS_{fusion} plots for the second cycle, the intercepts at −54.64 and −34.40 J K^{-1} mol^{-1} per CH_2 for odd- and even-chain homologues, respectively, are almost twice (−105.18 and −74.04 J K^{-1} mol^{-1} per CH_2, respectively) those for the first cycle and indicate that there is some reorganization of the structure after initial heating. The fact that these values, on average, are twice as large as those for the first cycle can be attributed to a possible reduction in the contribution from electrostatic interactions in the COO–Zn region, where the Zn–O bonds may be weaker after initial heating and cooling. Clearly, if the Zn–O bonds are weaker, then the distance between basal planes of the Zn^{2+} ion lattice is greater, thereby resulting in decreased repulsive electrostatic interactions, which leads to a less negative contribution to the melting process.

The thermodynamic data from the first cooling scans are given in Table 4; the data for the second cooling scans are almost similar to them, as in the case of data for the first and second heating scans. The isotropic liquid-to-Phase II transition temperatures are very similar in both cases and decrease with increasing chain length. However, the decrease is less dramatic when compared with the heating cycle and there is no apparent odd–even behavior. The absence of this odd–even behavior is because the molecular units have not completely reassembled on cooling from the isotropic liquid to Phase II and because Phase II is quite different from the room-temperature solid. Plots of ΔH_{trans} and ΔS_{trans} versus n_c result in reasonably good linear correlations, with slope and intercept values that are almost similar to the heating scans, and suggest that the heating–cooling cycle is fairly reversible.

Phase diagrams of transition temperature versus n_c for both first and second scans for odd- and even-chain homologues are shown in Fig. 4. It is evident that there is no odd–even variation for the intermediate transitions, but there is clearly an odd–even variation on melting into the isotropic liquid. It is seen that the number of phase transitions is related to the change in lattice structure of the compounds as chain length increases. Indeed, for the short-chain homologues, the lamellar bilayer lattice structure [14,15,17] is not as stable as the interdigitated bilayer lattice structure of the long-chain homologues [14,15–17].

3.3 Structural Reorganization: Role of Electrostatic Interactions During Melting

From the foregoing data, it is certain that on heating to the liquid and then cooling, there occurs some structural modification that alters the extent of the electrostatic interactions in the resulting room-temperature solid. Some evidence for the role of the electrostatic interactions in the melting process is provided by comparing the data from IR and X-ray analyses for the different compounds that were heated and then cooled back to room

Table 4. DSC thermodynamic data from the first cooling scan for zinc(II) *n*-alkanoates

	Lamellar crystal, L_C–Phase			Phase I–Phase II			Total		
Compound	T (±0.7 K)	ΔH_{trans} (±0.15 kJ mol^{-1})	ΔS_{trans} (±0.41 J K^{-1} mol^{-1})	T (±0.8 K)	ΔH_{trans} (±1.13 kJ mol^{-1})	ΔS_{trans} (±3.30 J K^{-1} mol^{-1})	ΔH_{total} (±1.57 kJ mol^{-1})	ΔS_{total} (±3.95 J K^{-1} mol^{-1})	Reference
ZnC_4	374.4	8.27	22.09	415.5	41.19	99.15	49.46	148.61	[5]
ZnC_5	374.6	7.74	20.66	411.5	36.42	88.52	44.16	132.68	This work
ZnC_6	374.9	17.63	47.03	405.7	48.18	118.77	65.81	184.58	[5]
ZnC_7	374.5	7.83	20.91	399.1	38.27	95.89	46.10	141.99	This work
ZnC_8	375.7	14.65	39.00	399.2	68.63	171.94	83.28	255.22	[5]
ZnC_9	371.7	7.11	19.13	399.3	76.70	192.11	83.81	275.92	This work
ZnC_{10}	370.3	13.50	36.46	396.4	80.63	203.43	94.13	297.56	[5]
ZnC_{11}	352.0	7.48	21.25	391.0	93.67	239.60	101.15	340.75	This work
ZnC_{12}	365.6	29.33	80.22	390.3	100.43	257.35	129.76	387.11	[5]
ZnC_{13}	377.1	11.71	31.05	388.8	88.88	228.63	100.59	329.22	This work
ZnC_{14}	350.8	24.43	69.65	386.5	125.80	325.53	150.23	475.76	[5]
ZnC_{15}	385.7	–	–	392.8	139.35	354.81	139.35	494.16	This work
ZnC_{16}	382.0	5.37	14.06	392.5	168.27	428.71	173.64	602.35	[5]
ZnC_{17}	381.0	8.92	23.41	392.9	163.93	417.28	172.85	590.13	This work
ZnC_{18}	–	–	–	390.2	173.99	445.96	173.99	619.95	[5]
ZnC_{19}	375.0	17.54	46.77	388.6	159.05	409.34	176.59	585.93	This work
ZnC_{20}	–	–	–	–	–	–	–	–	[5]

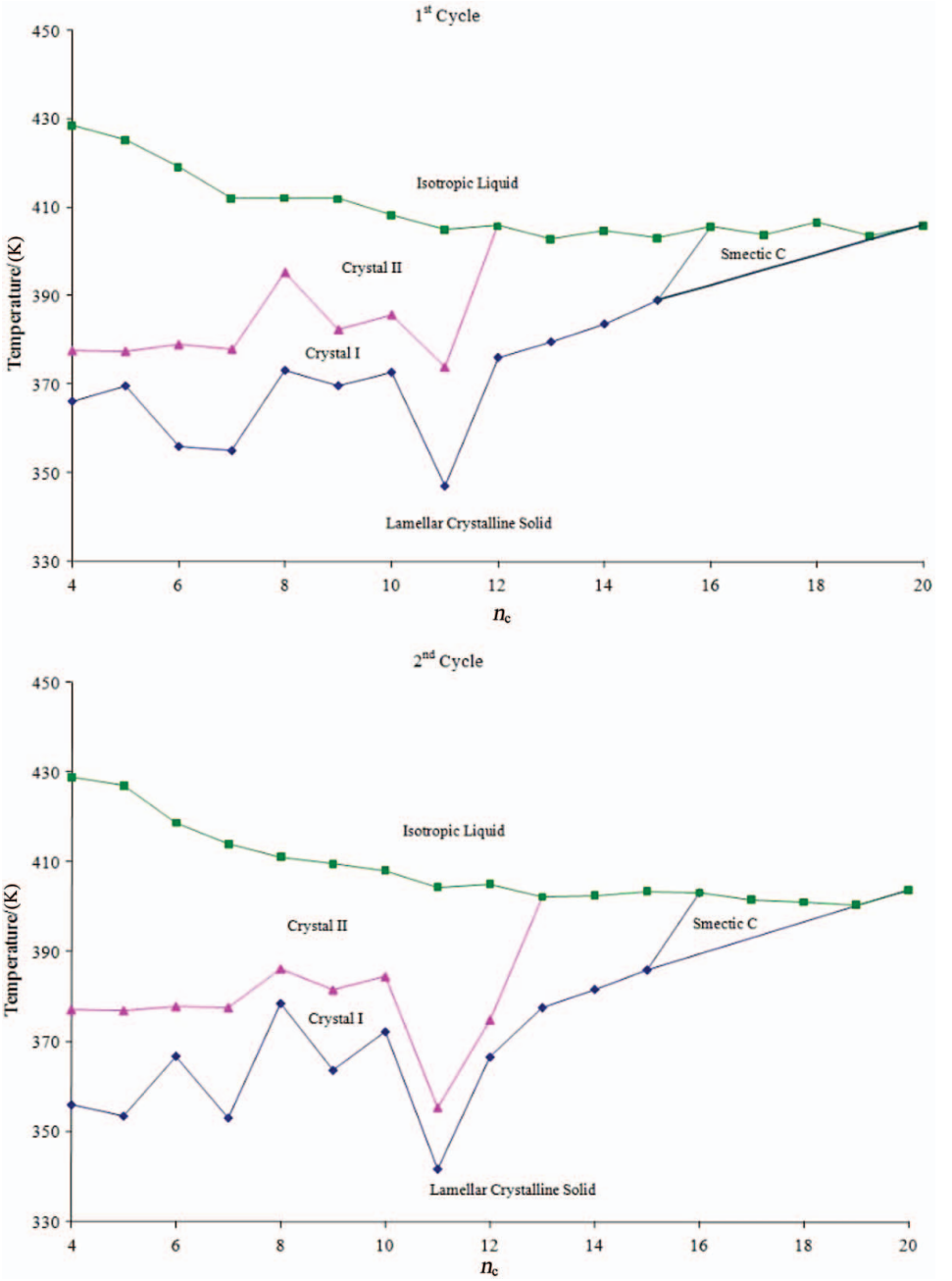

Figure 4. Phase diagrams of zinc(II) *n*-alkanoates for first and second heating cycles.

temperature (i.e., heated compounds) and for the unheated compounds. The IR spectra collected at room temperature for ZnC_5 and ZnC_{16}, representing short- and long-chain homologues, respectively, are shown in Fig. 5. The spectral data of asymmetric stretch (ν_a) of the COO^- group, symmetric stretch (ν_s) of the COO^- group, separation value

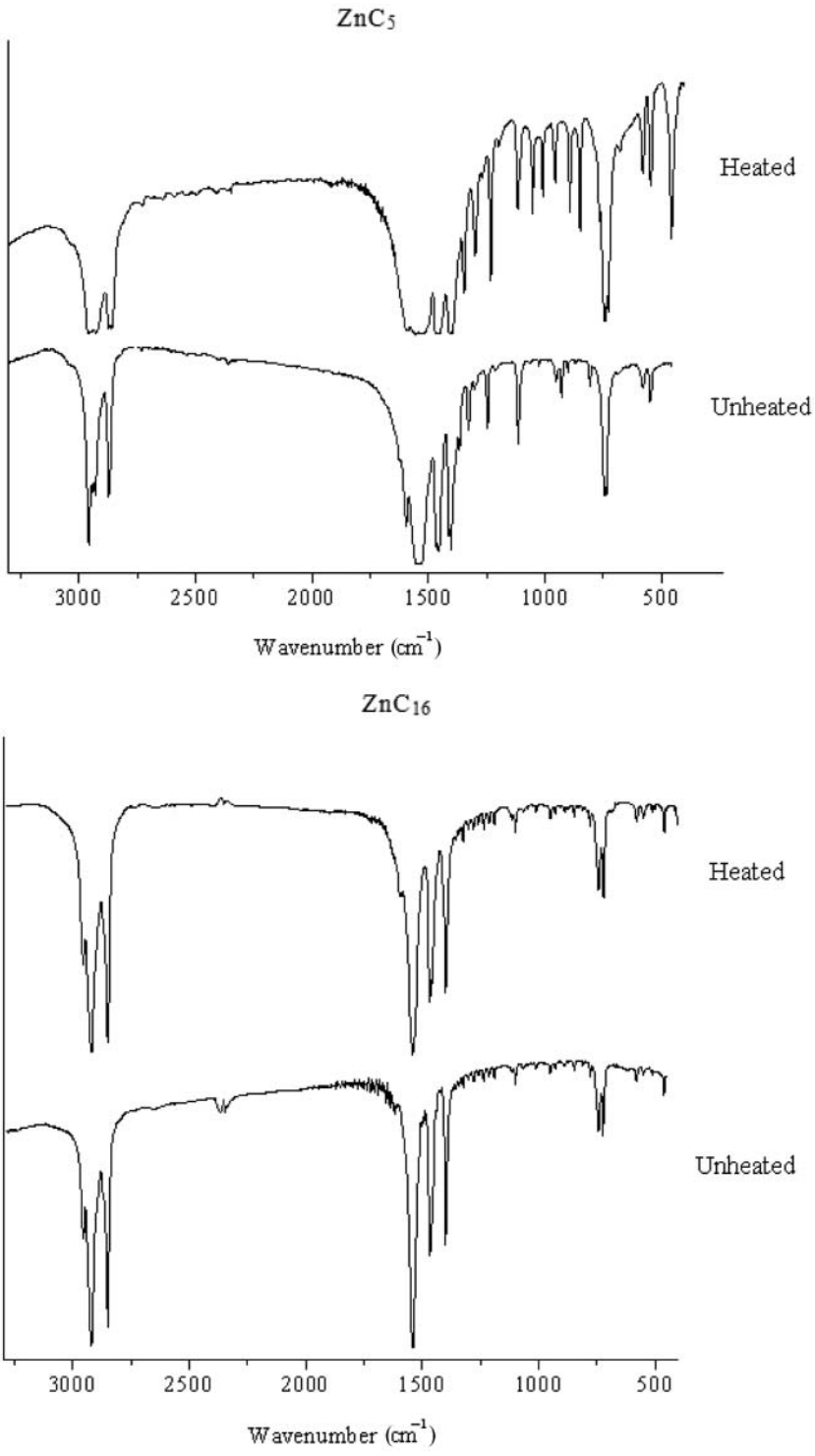

Figure 5. Comparative room-temperature IR spectra of heated and unheated ZnC_5 and ZnC_{16}.

Table 5. Room-temperature IR spectral data for both heated and unheated ZnC_5 and ZnC_{16}

	Selected COO^- bands and separation values (cm^{-1})			
Compound	ν_a(COO)	ν_s(COO)	$\Delta\nu$	ρ(COO)
ZnC_5 (U)	1549	1401	148	550
ZnC_5 (H)	1559	1396	163	556
ZnC_{16} (U)	1539	1398	141	550
ZnC_{16} (H)	1539	1398	141	549

Note. U = unheated; H = heated.

($\Delta\nu$(COO)), and rocking (ρ(COO)) are given in Table 5. For ZnC_5, they differ slightly for the heated compounds, indicating that the COO–Zn coordination structure is slightly less unsymmetrical when this compound is heated and then cooled. However, the change in these values for ZnC_{16} is negligible. These results suggest that there is no net change in the COO–Zn coordination structure and imply that this interaction is more or less the same.

On the other hand, the X-ray powder diffractograms shown in Fig. 6 are different for the heated and unheated compounds and indicate that there is some difference in the overall lattice arrangement. For the ZnC_5, the reflections are evenly spaced throughout the entire 2θ region for the unheated compounds, but only up to about $2\theta = 20^\circ$ for the heated compounds; the reflections at $2\theta = 20^\circ$–25° are indicative of side-chain interactions of the CH_2 groups with the layer planes [1,14,19]. For the ZnC_{16}, the reflections at $2\theta = 20^\circ$–25° are fewer but much more intense in the heated compounds and indicate an increase in side-chain interactions. This indicates that the hydrocarbon chains of the heated compounds are somewhat distorted compared with the unheated compounds, but still maintain the nearly all-*trans* conformation. Additionally, values of experimental lamellar spacing, d_{exp}, unit cell sides a, b, and c, along with tilt angles (r) for ZnC_5 and ZnC_{16}, (Table 6) are slightly larger for the heated compounds than for the unheated compounds and indicate that the chains are slightly less tilted. The slightly larger tilt angles of the hydrocarbon chains of the heated compounds indicate that the distance between basal planes of the Zn^{2+} ion lattice of all homologues is slightly larger, resulting in a small reduction in the repulsive interactions between the polar head groups where the lattice is slightly more relaxed and possibly more stable. This is in accord with the thermodynamic data, which suggest that the lattice structure has not significantly changed after heating to the isotropic liquid and

Table 6. X-ray powder data and angles of tilt, r (°) for heated and unheated ZnC_5 and ZnC_{16}

Compound	a (Å)	b (Å)	c (Å)	d_L (Å)	d_{exp} (Å)	r (°)
ZnC_5 (U)	28.26	4.27	8.28	16.48	28.28	59.09
ZnC_5 (H)	31.05	5.99	12.02	16.48	30.69	68.61
ZnC_{16} (U)	38.74	6.98	9.93	44.22	38.15	59.78
ZnC_{16} (H)	40.02	6.03	12.22	44.22	40.24	65.50

Note. U = unheated; H = heated.

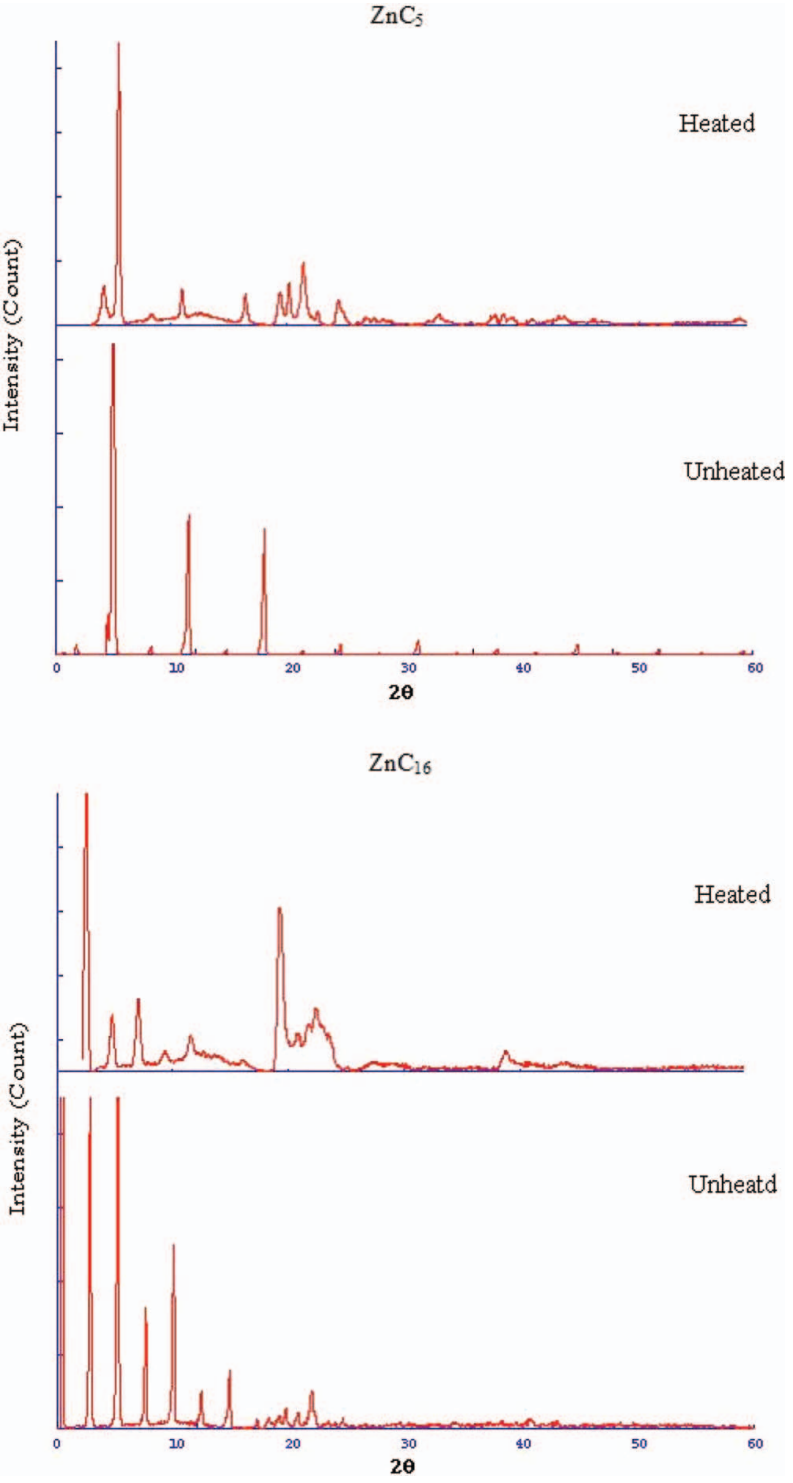

Figure 6. Comparative room-temperature X-ray powder diffractograms of heated and unheated ZnC_5 and ZnC_{16}.

then cooling back to room temperature. The slight change, however, is indicative of a slight reduction in the electrostatic interactions of the CH_3 group with the basal planes of the Zn^{2+} ion lattice.

3.4 Nature of the Melt

The formation of micellar aggregates in isotropic melts has been proposed for many metal carboxylates [1, 19, 20, 23, 25]. This means that the hydrocarbon chains retain some structural order and are not completely fused, i.e., the overall coordination structure is maintained. In the present case, the large ΔH_{fusion}, ΔS_{fusion}, ΔH_{total}, and ΔS_{total} indicate that the lamellar arrangement of hydrocarbon chains has completely fused and there is little or no formation of micellar aggregates at or after melting. Also, it is possible that there is some structural deformation of the polar head groups during melting.

Some evidence of the structure of the compounds in the molten state was provided by Ishioka et al. [26] in their study of the Zn^{2+} octadecanoate and by Mesubi [24], who studied the even-chain homologues. Their IR data indicated that the molten chains had liquid-like conformations and that the ν_a(COO) stretch was split into multiplets, suggesting a possible change in the coordination structure. In addition, EXAFS (extended X-ray absorption fine structure) data from Ishioka and co-workers [26] indicated that because the Zn–O bond distances were estimated to be 1.95 Å at room temperature and at melting, coordination numbers of 4.2 and 4.0, respectively, indicated that there was no change in the coordination structure. However, splitting of the ν_a(COO) bands into multiplets indicated that some structural change in the ionic region occurred, leading to a reduction in symmetry. They ascribed this change to geometrical distortion in the tetrahedral coordination structure of the Zn^{2+} and the COO^- ions, with the coordination number retained. Interestingly, their proposal was contradicted by Ekwunife et al. [27]. In their studies of electrical conductance of fused even-chain Zn(II) *n*-alkanoates, semi-logarithmic plots of specific conductivity versus inverse temperature were linear, where the slopes decreased very slightly with increasing chain length, having activation enthalpy, $H^{\#}$, for conduction of about 40 kJ mol^{-1}. They stated that the relatively small change in activation enthalpy, $\Delta H^{\#}$, in relation to chain length indicated that ions were formed in the melt and that they were the current carriers instead of aggregates. They postulated a dissociation equilibrium:

$$Zn(O_2CR)_2 \rightleftarrows Zn(O_2CR)^+ + RCO_2^- \rightleftarrows Zn^{2+} + 2RCO_2^-, \text{ where } R = (CH_2)_nCH_3.$$

It was reasonable to assume that Zn^{2+} carried the major fraction of the current compared with the other more bulky species. From our previous studies [14,15,17] of the structure in the solid phase, the compounds have shown a complex polymeric sheet-like network structure. Based on the molecular formula, $Zn_2[O_2C(CH_2)_nCH_3]_4$ and combining observations from Ishioka and co-workers [26] as well as Ekwunife and co-workers [27], a more likely dissociation equlibrium is proposed:

$$Zn_2(O_2CR)_4 \rightleftarrows Zn_2(O_2CR)_3^+ + RCO_2^- \rightleftarrows Zn(O_2CR)_2 + 2RCO_2^- + Zn^{2+}$$

This means that upon melting, the COO–Zn bonds get very distorted, weakened and finally break, thereby leading to large values of ΔH_{fusion}, ΔS_{fusion}, ΔH_{total}, and ΔS_{total}. The retention of the coordination number, as proposed by Ishioka et al. [26], could be as a result of the monomer species $Zn(O_2CR)_2$ (four oxygen atoms bonded to one Zn^{2+} atom) being present in the melt, but overall, the compounds are only slightly dissociated in the isotropic liquid, resulting in low ionic conductivity. This explains why the thermodynamic values

for the cooling cycles are almost similar, albeit slightly lower than those for the heating cycles, indicating that the heating–cooling process is fairly reversible, in accordance with the proposed equilibrium. Clearly, the isotropic liquid is a mixture of undissociated dimers and a few monomers as well as relatively small concentrations of COO^- anions and Zn^{2+} cations.

4. Conclusion

A combination of DSC data and microscopic phase textures for a series of odd-chain Zn(II) *n*-alkanoates indicates that these compounds display both enantiotropic and monotropic phase behaviors, similar to the even-chain homologues. Additionally, there is some relationship between the number of phases observed and the chain length. For example, there are three transitions for the short-chain, two for the medium-chain, and one for the long-chain homologues which are all ascribed to the difference in the lattice structures.

Interestingly, the odd–even behavior is observed in plots of ΔH_{fusion} and ΔH_{total}, and ΔS_{fusion} and ΔS_{total} versus chain length for the entire homologous series and suggests that the even-numbered hydrocarbon chains have a less negative contribution to the enthalpy of the melting process than their odd-chain counterparts because of a reduction in the repulsive electrostatic interactions due to greater packing efficiency in the lattice structure. The phase diagrams show that the odd–even behavior is not observed for the intermediate-phase transitions but only on fusion of the compounds.

Also, the linear increase in the values of ΔH and ΔS with chain length suggests that there is contribution from van der Waals interactions between the hydrocarbon chains and electrostatic interactions between the CH_3 group and the basal plane of the Zn^{2+} ion lattice, which are disrupted on heating, thus leading to an isotropic melt with very few or no micellar aggregates. There is significant distortion of the COO–Zn bond, resulting in some bond breaking and a mixture of undissociated dimers and a few monomers as well as relatively small concentrations of COO^- anions and Zn^{2+} cations. However, these species are in equilibrium, allowing for a reversible heating–cooling process which results in the dimer molecules retaining their layered polymeric molecular structures on cooling back to solid, albeit slightly altered, as evidenced from IR and powder X-ray diffraction data.

Acknowledgment

The authors express thanks to the School for Graduate Studies and Research, University of the West Indies, Mona, Jamaica, for funding this research.

References

[1] Akanni, M. S., Okoh, E. K., Burrows, H. D., & Ellis, H. A. (1992). *Thermochim. Acta*, *208*, 1–41.
[2] Ellis, H. A. (1981). *Thermochim. Acta*, *47*, 261–270.
[3] Burrows, H. D., & Ellis, H. A. (1982). *Thermochim. Acta*, *52*, 121–129.
[4] Ellis, H. A. (1986). *Mol. Cryst. Liq. Cryst.*, *139*, 281–290.
[5] Ellis, H. A. (1988). *Thermochim. Acta*, *130*, 281–288.
[6] Ellis, H. A., & De Vries, A. (1988). *Mol. Cryst. Liq. Cryst.*, *163*, 133–138.
[7] Ellis, H. A. (1997). *Mol. Cryst. Liq. Cryst.*, *308*, 111–120.
[8] Ellis, H. A., White, N. A. S., Hassan, I., & Ahmad, R. (2002). *J. Mol. Struct.*, *642*, 71–76.
[9] Ellis, H. A., White, N. A. S., Taylor, R. A., & Maragh, P. T. (2005). *J. Mol. Struct.*, *738*, 205–210.
[10] Taylor, R. A., Ellis, H. A., Maragh, P. T., & White, N. A. S. (2006). *J. Mol. Struct.*, *787*, 113–120.

[11] White, N. A. S. (2007). PhD thesis, University of the West Indies, Mona Campus, Jamaica, West Indies, 78–79.
[12] White, N. A. S., & Ellis, H. A. (2008). *J. Mol. Struct.*, *888* (1–3), 386–393.
[13] White, N. A. S., & Ellis, H. A. (2009). *Mol. Cryst. Liq. Cryst.*, *501*, 28–42.
[14] Taylor, R. A., & Ellis, H. A. (2007). *Spectrochim. Acta*, *68*, 99–107.
[15] Taylor, R. A., Ellis, H. A., & Maragh, P. T. (2009). *J. Mol. Struct*., *921*, 118–125.
[16] Taylor, R. A., & Ellis, H. A. (2009). *Liq. Cryst.*, *36*, 257–268.
[17] Taylor, R. A., Ellis, H. A., Maragh, P. T., & White, N. A. S. (2006). *J. Mol. Struct.*, *787*, 113–120.
[18] Neubert, M. E. (n.d.). *Identification of Liquid Crystal Textures, Liquid Crystal Institute*, Kent State University: Kent, OH.
[19] Marques, E. F., Burrows, H. D., & da Graça Miguel, M. J. (1998). *J. Chem. Soc. Faraday Trans.*, *94*, 1729–1736.
[20] Burrows, H. D. (1990). *The Structure, Dynamics and Equilibrium Properties of Colloidal Systems*, Kluwer Academic: The Netherlands.
[21] NIST Standard Reference Database. (2005). *NIST Chemistry WebBook (NIST Standard Reference Database No. 69)*, http://webbook.nist.gov/chemistry/form-ser.html
[22] Akanni, M. S., Okoh, E. K., Burrows, H. D., & Ellis, H. A. (1992). *Thermochim. Acta*, *208*, 1–41.
[23] Konkoly-Thege, I., Ruff, I., Adeosun, S. O., & Sime, S. J. (1978). *Thermochim. Acta*, *24*, 89–96.
[24] Mesubi, M. A. (1982). *J. Mol. Struct.*, *81*, 61–71.
[25] Burrows, H. D. (1992). *Molecular Liquids: New Perspectives in Physics and Chemistry*, Kluwer Academic: The Netherlands.
[26] Ishioka, T., Maeda, K., Watanabe, I., Kawauchi, S., & Harada, M. (2000). *Spectrochim. Acta Part A*, *56*, 1731–1737.
[27] Ekwunife, M. E., Nwachukwu, M. U., Rinehart, F. P., & Sime, S. J. (1975). *J. Chem. Soc. Faraday Trans. 1*, *71*, 1432–1446.